ACCSCIENCE PUBLISHING

International Journal of Bioprinting

RESEARCH ARTICLE

In vivo evaluation of a 3D-printed personalized temporomandibular joint condylar prosthesis with an elastic layer for hemiarthroplasty

Junqi Jiang[1†], Qingxiang Li[1†], Zhiwei Jiao[2], Kenan Chen[1], Junlin Wang[3], Bingxue Cheng[4], Chuanbin Guo[1*], and Xiangliang Xu[1*]

[1]Department of Oral and Maxillofacial Surgery, National Center of Stomatology and National Clinical Research Center for Oral Diseases and National Engineering Research Center of Oral Biomaterials and Digital Medical Devices and Beijing Key Laboratory of Digital Stomatology and Research Center of Engineering and Technology for Computerized Dentistry, Ministry of Health and NMPA Key Laboratory for Dental Materials, Peking University School and Hospital of Stomatology, Beijing, China

[2]College of Mechanical and Electrical Engineering, Beijing University of Chemical Technology, Beijing, China

[3]Department of Oral and Maxillofacial Surgery, Stomatological Hospital, School of Stomatology, Southern Medical University, Guangzhou, Guangdong, China

[4]State Key Laboratory of Tribology in Advanced Equipment, Tsinghua University, Beijing, China

[†]*These authors contributed equally to this work.*

***Corresponding authors:**
Xiangliang Xu
(kqxxl@126.com);
Chuanbin Guo
(guodazuo@sina.com)

Citation: Jiang J, Li Q, Jiao Z, *et al*. *In vivo* evaluation of a 3D-printed personalized temporomandibular joint condylar prosthesis with an elastic layer for hemiarthroplasty. *Int J Bioprint*. 2026;12(4):026210208. doi: 10.36922/IJB026210208

Received: May 23, 2026

Revised: June 21, 2026

Accepted: June 26, 2026

Published online: July 2, 2026

Abstract

Reconstructing severe temporomandibular joint defects remains a significant challenge in oral and maxillofacial surgery. This study evaluated the *in vivo* performance of a novel, 3D-printed personalized temporomandibular joint (TMJ) condylar prosthesis featuring an integrated elastic functional layer in a goat model. Conventional rigid metal and ultra-high-molecular-weight polyethylene (UHMWPE) prostheses often lead to stress shielding and contralateral joint degeneration due to a mechanical mismatch with the native articular disc. To address these limitations, unilateral hemi-TMJ reconstructions were performed on four adult male goats using a custom prosthesis that combined a porous Ti6Al4V stem with a three-dimensionally printed UHMWPE/high-density polyethylene (HDPE) composite elastic layer. Over a six-month follow-up, clinical, radiographic, and histological parameters were evaluated. All animals survived without serious complications. Maximum passive mouth opening and lateral excursion ranges successfully returned to levels comparable to preoperative baselines, while masticatory efficiency stabilized after an initial postoperative decline. Hepatic and renal function metrics confirmed the material's systemic biosafety. Computed tomography (CT) and micro-CT imaging verified stable prosthetic positioning, robust osseointegration, and bone matrix ingrowth into the porous metallic scaffold. Histological analysis revealed the formation of a beneficial "synovial-like" membrane on the elastic substrate surface, supported by significantly elevated local expression of the regenerative cytokine transforming growth factor beta, as measured by enzyme-linked immunosorbent assay. These findings suggest that the elastic design promotes favorable initial stability, good biocompatibility, and vital functional recovery. The observed synovial metaplasia provides a promising protective mechanism that minimizes wear and prevents heterotopic ossification, offering strong preclinical evidence for the use of elastic configurations in advanced TMJ arthroplasty.

Keywords: Temporomandibular joint prosthesis; Three-dimensional printing; Elastic functional layer; Synovial metaplasia; *In vivo* evaluation

1. Introduction

The temporomandibular joint (TMJ) is a unique and complex articulation critical for mastication, speech, and facial expression. For patients suffering from severe end-stage TMJ disorders resulting from trauma, ankylosis, or extensive tumor resection, total TMJ replacement has become a viable and reliable reconstructive option.[1,2] Currently, clinical practice predominantly relies on two major commercially available TMJ prostheses: the stock or custom-made Zimmer Biomet systems (Biomet Microfixation, United States) and the custom-made TMJ Concepts systems (TMJ Concepts Inc., United States).[3] Although traditional alloplastic TMJ prostheses offer immediate and vital structural support, they are predominantly fabricated from rigid materials, such as titanium alloys and standard ultra-high-molecular-weight polyethylene (UHMWPE). These materials possess an elastic modulus significantly greater than that of the native mandible, invariably inducing stress-shielding effects.[4] Consequently, this biomechanical mismatch can lead to periprosthetic bone resorption and severe complications, including screw loosening and implant failure.[5] Furthermore, this rigidity partially explains the current clinical contraindication to hemiarthroplasty, as high-modulus prostheses can cause severe wear and structural damage to the opposing natural glenoid fossa and articular disc.[6] Although total TMJ replacement is technically more demanding than hemiarthroplasty, total joint replacement remains the clinical standard regardless of glenoid fossa compromise.[7,8] To overcome the anatomical mismatch frequently encountered with off-the-shelf standard sizes, patient-specific total joint reconstruction using computer-aided design and manufacturing or three-dimensional (3D) printing has expanded significantly, enabling complex geometries that precisely mirror individual bony contours, thereby improving initial fixation and safeguarding vital neurovascular structures.[9,10] However, existing prosthetic designs primarily focus on replacing the rigid bony structures. They overlook the distinct biomechanical roles of the native articular disc and cartilage. The natural articular disc is integral to the complex movements of the TMJ, providing essential shock absorption, lubrication, and stress distribution.[11] While recent polyurethane or acellular disc prostheses exhibit certain dynamic behaviors, they still lack validation in large-animal models.[12,13] Ultimately, Xu *et al.*[14] suggest that prostheses lacking physiological elasticity can adversely alter the biomechanical behavior and long-term health of the contralateral joint.

Recent advancements in 3D printing and biomaterials offer unprecedented opportunities to address these biomechanical limitations through biomimetic design. Although a 3D-printed customized polyetheretherketone TMJ condylar prosthesis, developed by Guo *et al.*[15] showed promising *in vitro* validation, its wear resistance falls short compared to UHMWPE. Additionally, patient-specific musculoskeletal modeling has been successfully applied to design personalized 3D-printed titanium condylar prostheses, which actively reduce screw and bone stresses during physiological clenching.[16] Our group has previously developed a novel elastic TMJ condylar prosthesis. This innovative design integrates a porous Ti6Al4V stem with an elastic functional layer (EFL) composed of a 3D-printed UHMWPE/high-density polyethylene (HDPE) composite. This EFL is specifically engineered to mimic the cushioning and load-distributing functions of the natural articular disc. *In vitro* studies have confirmed its optimized elastic modulus, excellent mechanical compatibility, and potential to mitigate stress concentrations.[17] Building directly upon our prior *in vitro* design and fabrication framework, the current study represents a critical incremental advancement by providing the first *in vivo* validation in large animals of this elastic functional layer configuration.

To bridge the gap between *in vitro* promise and clinical translation, rigorous *in vivo* evaluation is imperative.[18] Large animal models, particularly goats, are considered the gold standard for TMJ research due to the distinct anatomical and biomechanical similarities between their TMJ structures and those of humans.[19] Mommaerts *et al.*[20] verified a novel TMJ prosthesis that permits the reinsertion and integration of the lateral pterygoid muscle into the prosthesis in a goat model. Therefore, the present study aims to conduct a comprehensive *in vivo* assessment of this novel elastic prosthesis using a goat hemi-TMJ replacement model. We evaluated its surgical feasibility, short- to medium-term biosafety, mechanical stability, and efficacy in restoring mandibular function. We hypothesized that this design would not only provide sufficient mechanical support and physiological elasticity, but also preserve joint function by preventing adverse wear on native tissues and promoting favorable osseointegration.

2. Materials and methods

2.1. Ethical statement

All procedures were approved by the Institutional Animal Care and Use Committee of Peking University School of Stomatology (Approval No. LA2020286) and were conducted in strict accordance with national guidelines for the care and use of laboratory animals.

2.2. Research subjects and computed tomography acquisition

Four healthy adult male goats (aged 1.5–2 years, weighing 60–70 kg) were selected for this study (Beijing Jinmuyang Experimental Animal Breeding Co., Ltd.). Inclusion criteria included good nutritional status, absence of systemic diseases, and normal dentition without missing teeth or malocclusion. Following a two-week acclimatization period in the animal facility, preoperative computed tomography (CT) scans were performed. Anesthesia was induced via intramuscular injection of Zoletil (tiletamine/zolazepam) and xylazine (0.14 mL/kg). A 16-slice CT scan (uCT510, United Imaging, China) was conducted with a slice thickness of 0.6 mm, and data were exported in DICOM format. Scans were acquired in four mandibular positions: closed mouth, passive maximum mouth opening, passive maximum left lateral excursion, and passive maximum right lateral excursion. During anesthesia recovery, respiration was carefully monitored to prevent airway obstruction.

2.3. Prosthesis design and fabrication

A subject-specific TMJ condylar prosthesis was designed from preoperative CT data using a digital workflow that included Geomagic Wrap 17.0 (3D Systems, United States), SolidWorks (Dassault Systèmes, France), and Element (nTopology Inc., United States). The prosthesis comprised two primary components:

- The Ti6Al4V mandibular ramus stem, manufactured via selective laser melting, utilized a topologically optimized porous scaffold to mitigate the stress-shielding effect, thereby preventing periprosthetic bone resorption. Concurrently, an inlay rod and an onlay plate were designed to provide immediate mechanical stability against the remaining mandible.[21]
- The EFL was composed of a UHMWPE/HDPE composite (4:6 mass ratio, selected based on our prior optimization study demonstrating its superior balanced elasticity and wear resistance),[17] fabricated using our self-developed fused deposition modeling 3D printing system. Crucially, the composite material exhibits excellent biocompatibility, as reported by Shokrgozar *et al.*[22] The key fused deposition modeling printing parameters were set as follows: nozzle temperature of 240 °C, layer thickness of 0.2 mm, and a printing speed of 350 mm/min. The internal porous scaffold of this layer was designed with eight staggered layers and a 0°/90° infill pattern to achieve an optimized elastic modulus.[17]

The two components were mechanically integrated using a custom "mortise-tenon" joint and subsequently welded. The articular surface was polished to a final roughness of Sa < 2 μm, which was verified by white light interferometry (Figure 1).

2.4. Animal model and surgical procedure

Following a six-hour preoperative fasting period, anesthesia was induced identically to the CT acquisition protocol. The surgical site over the right TMJ was shaved, prepared, and draped under standard aseptic conditions.

An incision was made along the posterior border of the mandible. The anterior attachment of the parotid gland was carefully dissected and retracted posteriorly to protect the facial nerve. The mandibular ramus and condyle were exposed, and the condyle was meticulously dissected from the articular disc to allow full mobilization. According to the preoperative plan, a condylectomy was performed 15 mm from the condylar apex using a powered surgical saw. Sharp bony edges were smoothed to finalize the hemi-TMJ defect model.

For prosthesis implantation, a fixation hole was drilled perpendicular to the cross-section of the mandibular ramus to accommodate the inlay stem. The custom 3D-printed prosthesis was inserted into the defect, ensuring the onlay plate adapted seamlessly to the lateral contour of the mandible. Rigid fixation was achieved using titanium screws at the pre-planned sites. The surgical site was irrigated with sterile saline. The periosteum was left unsutured, while the subcutaneous tissue and skin were closed in layers. A surgical drain was placed and subsequently removed 24 hours postoperatively (Figure 2).

Postoperative care included intramuscular administration of penicillin sodium (1.6×10^6 U/day) for one week as infection prophylaxis, and lidocaine for analgesia. The goats were maintained on a soft/liquid diet for the first week. Feeding behavior and general health were monitored daily.

2.5. Postoperative observation and tissue sampling

At the designated end of the six-month observation period, prior to euthanasia, the body weight of each goat was recorded. Under induction anesthesia (0.14 mL/kg Zoletil/xylazine), postoperative CT imaging was conducted in the

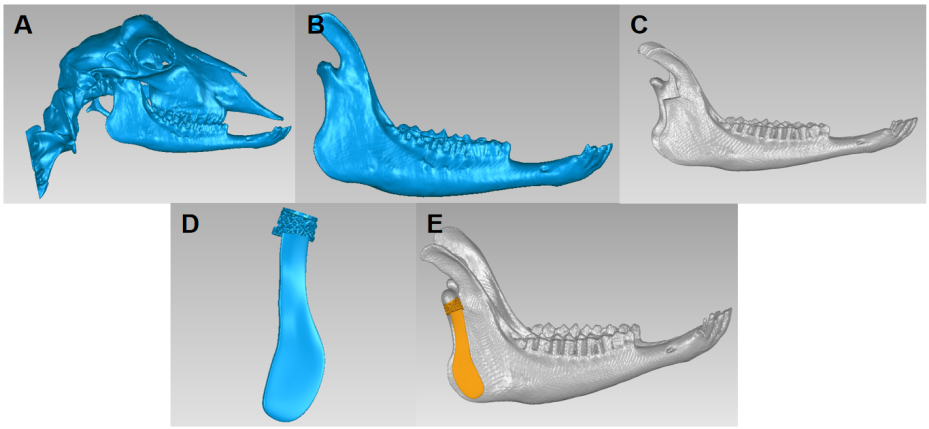

Figure 1. Digital design workflow of the elastic temporomandibular joint (TMJ) condylar prosthesis for goats. (A) Goat craniomandibular model. (B) Mandibular model. (C) Right TMJ defect model. (D) Mandibular ramus stem component (Ti6Al4V) model. (E) Final assembly model showing the integrated elastic TMJ condylar prosthesis *in situ*.

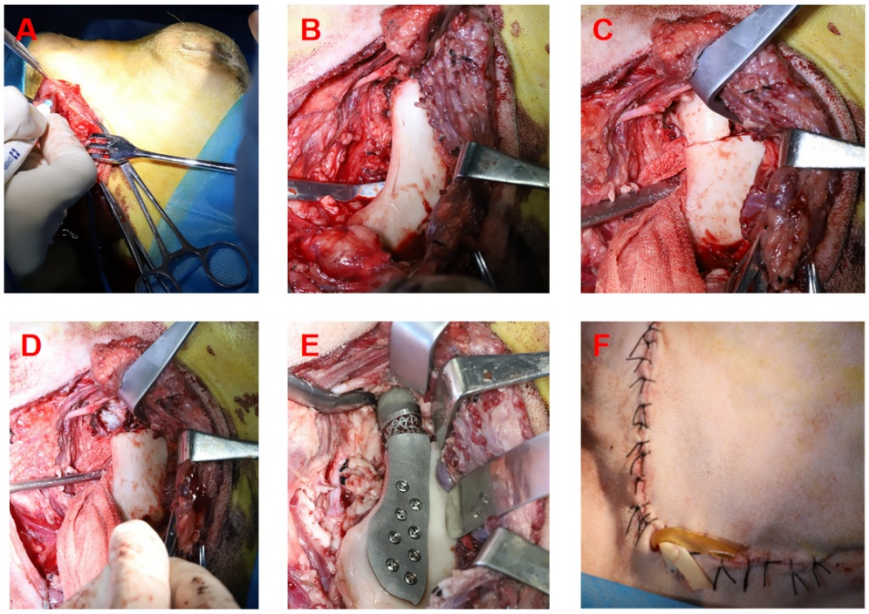

Figure 2. Surgical procedures for the implantation of the temporomandibular joint (TMJ) condylar prosthesis in a goat model. (A) Skin and subcutaneous tissue incision. (B) Surgical exposure of the mandibular ramus. (C) Osteotomy performed along the preplanned line using a power-tool system. (D) Resection of the native condyle. (E) Implantation and fixation of the personalized prosthesis. (F) Layered wound closure and placement of a surgical drain.

aforementioned four mandibular positions. The surgical sites were then prepared, and the animals were humanely euthanized.

Soft tissues surrounding the right TMJ were dissected to expose the prosthesis. Tissue samples closely adhering to the anterior, posterior, medial, and lateral aspects of the prosthetic condyle were harvested in duplicate, labeled, and snap-frozen at −80 °C for molecular biological analysis. Subsequently, the TMJ prosthesis *in situ*, along with adjacent bone tissue within a 1 cm radius, was excised *en bloc* and fixed in formalin for histological evaluation. Contralateral native TMJs (left side) were similarly dissected, and corresponding soft tissue samples were collected as within-animal controls.

2.6. Evaluation protocol

Comprehensive evaluations were conducted preoperatively, and at two weeks, one month, and six months postoperatively:

(i) Clinical observation: General health, wound healing, and signs of complications (e.g., infection, wound dehiscence, or prosthesis exposure) were routinely monitored.
(ii) Maximum passive mouth opening (MPMO): The maximum distance between the incisal edges of the upper and lower central incisors during passive opening was measured using a steel caliper.
(iii) Maximum lateral range of movement: The maximum horizontal displacement of the mandible to the left and right was recorded.
(iv) Masticatory efficiency: The time required for each goat to completely consume 100 g of standardized feed (dry pelletized forage, 5 mm diameter, 12% moisture content) was documented.
(v) Serum biochemistry: Blood samples were collected to evaluate liver and kidney function using an automatic biochemical analyzer (Catalyst One, IDEXX, United States). Metrics included alanine aminotransferase (ALT), alkaline phosphatase (ALP), total protein (TP), albumin (ALB), creatinine (CR), and blood urea nitrogen (BUN).[23]
(vi) Macroscopic CT analysis: Symmetrical comparisons between the prosthetic and healthy joints were performed. Measurements included ramus height (RH; condylar apex to mandibular angle), mandibular body length (ML; mandibular angle to mental protuberance), condyle–incisor distance (CI; condylar apex to mandibular central incisor), and submental–condyle distance (BC).[24]
(vii) Micro-CT analysis: Explanted bone prosthesis blocks were scanned using a micro-CT system (Inveon, Siemens, United States) at 60 kV and 220 μA, with an exposure time of 500 ms and a voxel size of 8.82 μm. Images were reconstructed via the Inveon Research Workplace (version 4.0) to evaluate prosthetic fit, bone ingrowth, and structural integrity compared to the healthy joint.
(viii) Histological staining and cytokine analysis: Hard tissue specimens were processed and sectioned, followed by staining with hematoxylin and eosin (H&E), Masson's trichrome, and toluidine blue to assess osseointegration and tissue response. All images were obtained with an optical microscope (Olympus BX53, Japan). Additionally, enzyme-linked immunosorbent assay (ELISA; MEIMIAN, China) was employed to quantify local inflammatory and remodeling cytokines (interleukin [IL]-1α, IL-1β, IL-8, IL-10, tumor necrosis factor alpha, interferon gamma, transforming growth factor beta [TGF-β]) in the peri-prosthetic soft tissues. All tissue specimens were standardized to a wet weight of 50 mg, and final cytokine concentrations were strictly normalized against the total protein content of the respective supernatant.

To eliminate observer bias, all postoperative functional assessments (MPMO, maximum lateral range of movement, masticatory efficiency), radiographic measurements, and histological evaluation were performed by two independent investigators who were completely blinded to the surgical protocol and animal identity. Inter-observer discrepancies were resolved by consensus.

2.7. Statistical analysis

Statistical analysis was performed using GraphPad Prism 6 (GraphPad Software Inc., United States). Data are expressed as the mean ± standard deviation (SD). Following descriptive statistical evaluation, intra-group pairwise comparisons were performed using the paired Student's *t*-test. $p < 0.05$ was considered statistically significant.

3. Results

3.1. General observations

All four experimental animals survived the entire experimental period and successfully completed the study protocol, including clinical observations, specimen collection, and radiographic imaging. No postoperative complications, such as infections, trismus, or prosthesis exposure, were observed.

3.2. Masticatory efficiency

Masticatory efficiency declined significantly postoperatively across all subjects compared with the preoperative baseline. At the six-month postoperative mark, the average chewing time required to consume 100 g of standardized feed increased by 8.25 ± 2.99 minutes relative to preoperative levels, representing a statistically significant reduction in efficiency ($p < 0.05$). Notably, masticatory efficiency stabilized after the initial healing phase, showing no statistically significant differences among the two-week, one-month, and six-month postoperative time points ($p > 0.05$) (Figure 3).

3.3. Maximum passive mouth opening

At six months postoperatively, the MPMO in two goats returned to preoperative levels, while the remaining two goats exhibited a slight decrease compared to baseline. There were no statistically significant differences in MPMO between the two-week and six-month postoperative intervals compared to the preoperative baseline, indicating excellent preservation of vertical mandibular mobility ($p > 0.05$) (Figure 4).

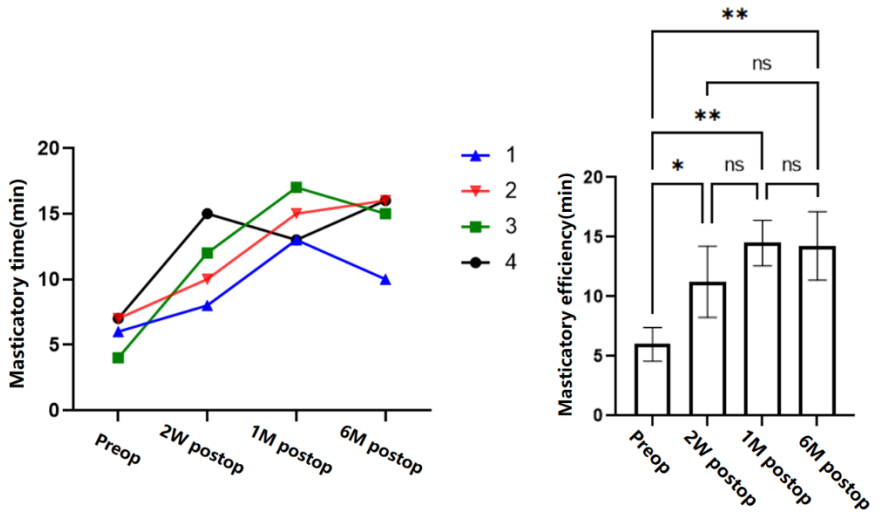

Figure 3. Changes in masticatory efficiency in four goats following temporomandibular joint (TMJ) replacement: Mean values and inter-group comparisons at different time points. The graph displays the time required for mastication (minutes) for the four experimental goats (1–4) at preoperative (Preop), two-week postoperative (2W postop), one-month postoperative (1M postop), and six-month postoperative (6M postop) intervals. Statistical analysis was performed using paired *t*-tests for pairwise comparisons. ns: $p > 0.05$; *$p < 0.05$; **$p < 0.01$.

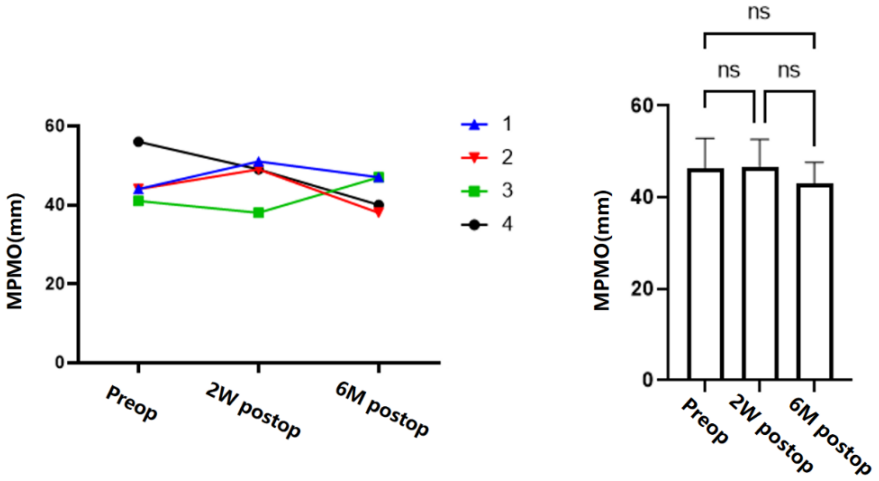

Figure 4. Changes in maximum passive mouth opening (MPMO) in the goat model: Mean values and inter-group comparisons at different time points. The graph displays the individual trends of MPMO (mm) for the four experimental goats (1–4) at preoperative (Preop), two-week postoperative (2W postop), and six-month postoperative (6M postop) intervals. Statistical analysis was performed using paired *t*-tests for pairwise comparisons. ns: $p > 0.05$.

3.4. Maximum lateral range of movement

All animals effectively retained lateral mandibular mobility postoperatively. At two weeks postoperatively, the right lateral excursion range was significantly reduced compared to preoperative levels ($p < 0.05$). However, by the six-month follow-up, both left and right lateral excursions had recovered to baseline levels, with no statistically significant differences ($p > 0.05$), thereby confirming functional restoration of lateral excursion (Figure 5).

3.5. Hepatic and renal function metrics

The levels of ALT, ALP, TP, ALB, CR, and BUN were measured preoperatively, at two weeks, and at six months postoperatively. The normal reference ranges for these parameters are as follows: ALT (23–44 U/L), ALP (26.9–283.3 U/L), TP (57–81 g/L), ALB (21–37 g/L), CR (53–159 μmol/L), BUN (1.8–7.1 mmol/L). All parameters remained within physiological ranges throughout the study period, indicating no systemic toxicity and the safety of the implanted materials (Figure 6).

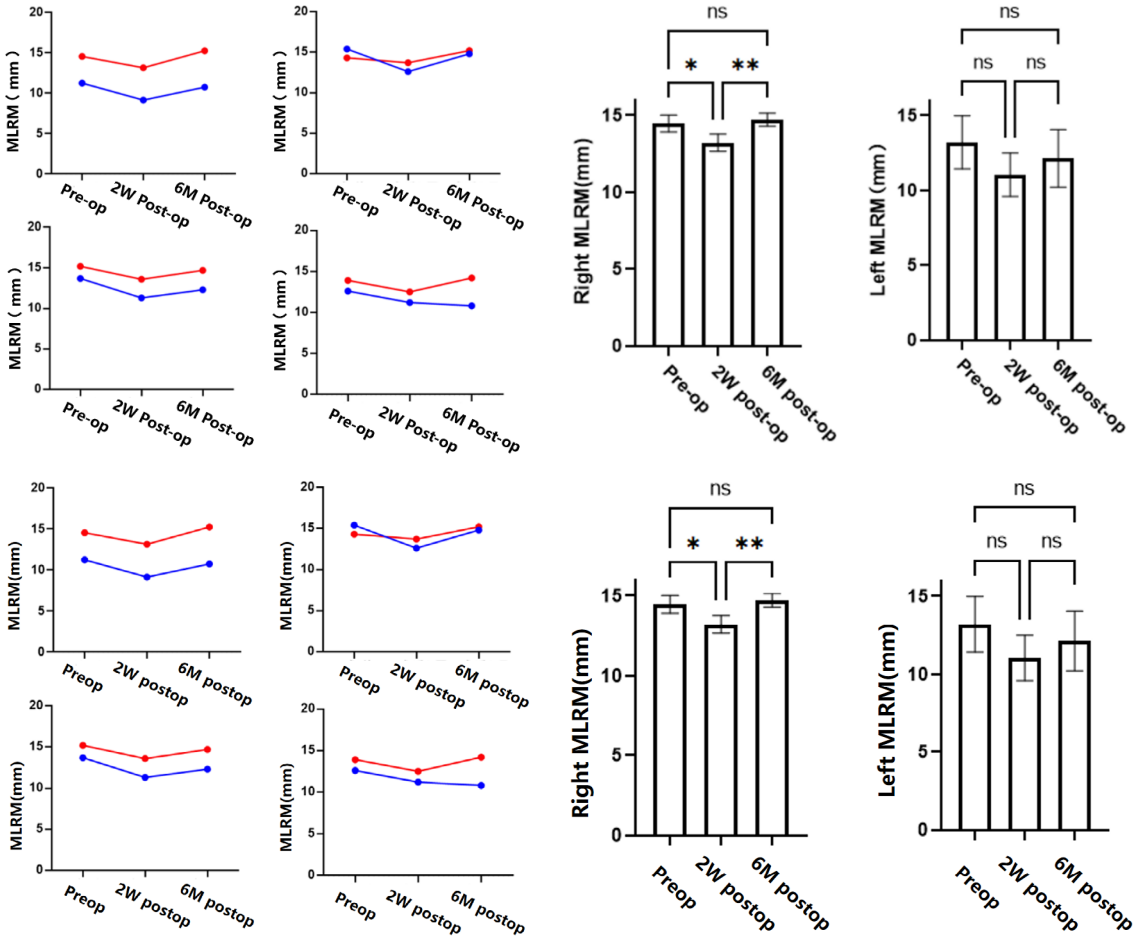

Figure 5. Changes in the maximum lateral excursion range in four experimental goats: Mean values and inter-group comparisons at different time points. The red lines represent the range of left lateral excursion, and the blue lines represent the range of right lateral excursion. Data were recorded at preoperative, two-week postoperative, and six-month postoperative intervals. Statistical analysis was performed using paired *t*-tests for pairwise comparisons. ns: $p > 0.05$; *$p < 0.05$; **$p < 0.01$.
Abbreviation: MLRM: Maximum lateral range of movement.

3.6. Three-dimensional morphometric and micro-computed tomography analysis

No significant differences were observed in RH, ML, CI, and BC between the two-week and six-month postoperative intervals ($p > 0.05$). All deviations in these parameters were within 2 mm, suggesting structural stability of the prosthesis (Figure 7). CT imaging showed the TMJ prosthesis was in a stable position (Figure 8). Micro-CT imaging of the four specimens at the six-month mark demonstrated a tightly apposed interface between the prosthesis and the mandible, with no signs of loosening or gaps. Notably, increased radiopaque signal intensity (indicating higher density) was observed within the internal porous metal scaffold, suggesting potential bone ingrowth and integration into the structure. The bone architecture and mineral density of the contralateral healthy joints remained within physiological limits (Figure 9).

3.7. Histological evaluation

Histological analysis using H&E, toluidine blue, and Masson's trichrome staining (10× magnification) revealed the formation of a synovium-like acellular structure on the surface of the condylar prosthesis six months postoperatively (Figure 10). The joint cavity remained patent with no evidence of fibrous adhesion. Furthermore,

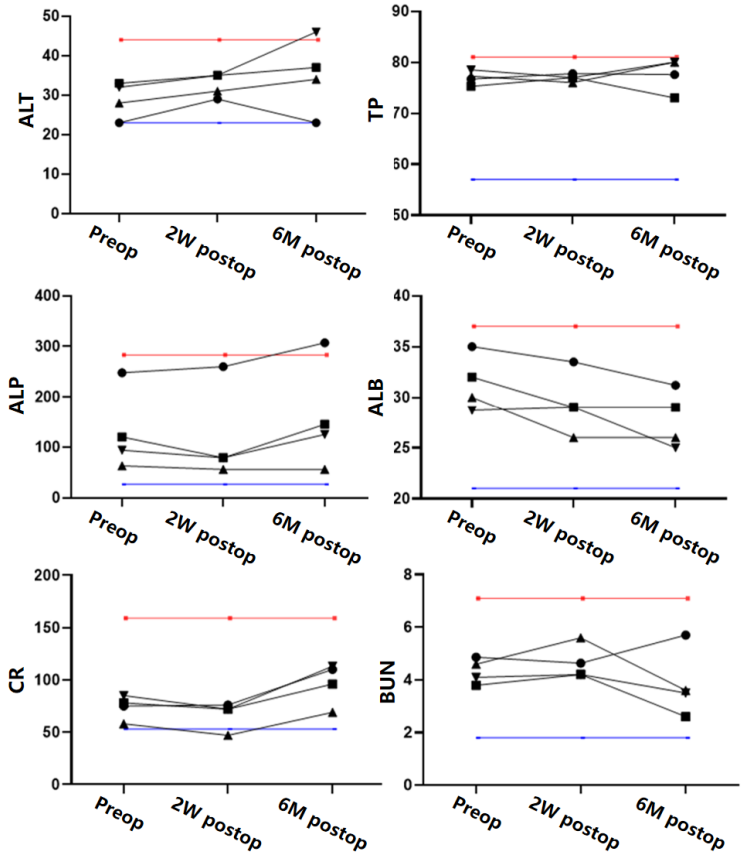

Figure 6. Longitudinal assessment of hepatic and renal function indicators in goats. The graphs show the levels of ALT, TP, ALP, ALB, CR, and BUN at preoperative (Preop), two-week postoperative (2W Postop), and six-month postoperative (6M Postop) stages. The red horizontal lines indicate the upper limit of the physiological reference range, while the blue horizontal lines indicate the lower limit. All parameters for the four experimental goats remained within normal physiological limits throughout the study period.
Abbreviations: ALB: Albumin; ALP: Alkaline phosphatase; ALT: Alanine aminotransferase; BUN: Blood urea nitrogen; CR: Creatinine; TP: Total protein.

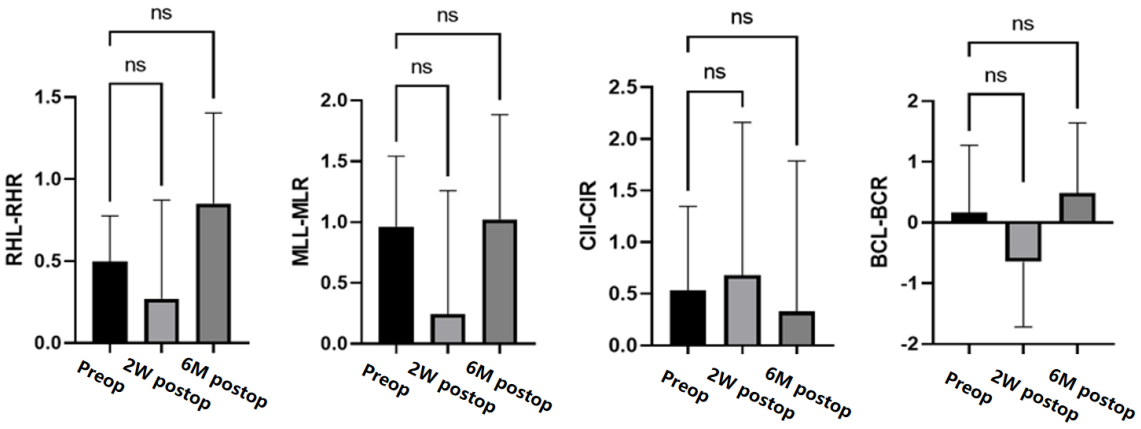

Figure 7. Comparison of bilateral symmetry in RH, ML, CI, and BC at different time points. The bar graphs represent the differences between the left and right sides for each parameter (RH, ML, CI, and BC) at preoperative, two-week postoperative, and six-month postoperative intervals. Statistical analysis was performed using paired t-tests for pairwise comparisons. ns: $p > 0.05$.
Abbreviations: BC: Submental–condyle distance; CI: Condyle–incisor distance; L: Left; ML: Mandibular body length; R: Right; RH: Ramus height.

the porous elastic scaffold maintained structural integrity, with visible intramedullary bone matrix formation.

3.8. Enzyme-linked immunosorbent assay results

Enzyme-linked immunosorbent assay showed that TGF-β levels in the affected joint group were significantly higher than in the healthy control group ($p < 0.05$). In contrast, no statistically significant differences were observed in the levels of IL-1α, IL-1β, IL-8, IL-10, tumor necrosis factor alpha, and interferon gamma between the test and control groups ($p > 0.05$) (Figure 11). This cytokine profile indicates a localized tissue response characterized by elevated TGF-β upregulation.

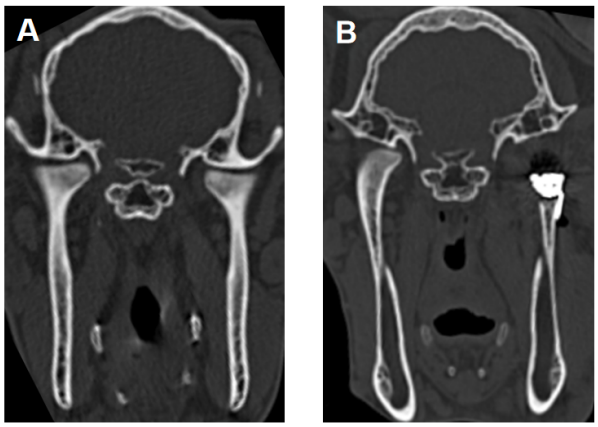

Figure 8. Coronal computed tomography (CT) images. (A) Preoperative CT scan. (B) Postoperative CT scan at six-month follow-up.

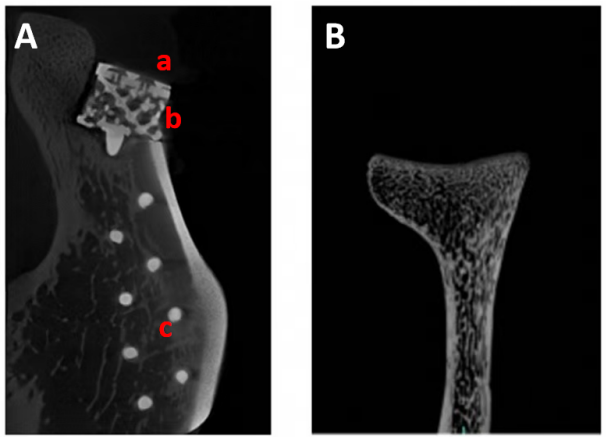

Figure 9. Micro-computed tomography (CT) images of the operated and contralateral temporomandibular joints (TMJs). (A) Representative Micro-CT image of the operated side showing the prosthesis: (a) the three-dimensional-printed elastic porous layer, (b) the metallic scaffold structure (Ti6Al4V), and (c) the fixation screws. (B) Micro-CT image of the contralateral TMJ as a baseline.

4. Discussion

The clinical management of severe end-stage TMJ disorders via hemiarthroplasty has historically been constrained by the high elastic modulus of traditional rigid materials, which invariably causes catastrophic mechanical wear on the native glenoid fossa and alters contralateral joint kinematics.[25,26] By evaluating our independently developed EFL prosthesis in a goat model, this study demonstrates that introducing localized mechanical compliance can fundamentally bridge this structural mismatch. The successful recovery of mandibular mobility, stable spatial alignment, and preserved tissue architecture observed within six months suggest that mitigating interfacial rigidity facilitates functional joint adaptation without inducing immediate structural failure or periprosthetic gaps. This biomechanically inspired approach presents a stark contrast to traditional custom-made systems that rely strictly on rigid metals or solid UHMWPE, offering a viable preclinical strategy to preserve the natural fossa and reduce surgical invasiveness.

Histological analysis revealed the formation of characteristic "synovial-like" structures on the surface of the EFL, a phenomenon known as synovial metaplasia (SM). First reported on the surfaces of silicone TMJ implants in 2012,[27] the exact mechanism of SM remains to be fully elucidated. It is hypothesized that SM arises from a combination of the material's inherent properties and the long-term biological response to implantation. Mechanical stress is considered a critical inductive factor;[28, 29] for instance, Drachman *et al.*[30] demonstrated that synovial tissue fails to develop normally during embryonic stages in the absence of mechanical stimulation. While the exact etiology of SM in TMJ reconstruction remains to be fully elucidated, mechanical stress and biomaterial surface properties are considered critical factors in its induction. In this study, the formation of a "synovial-like" membrane on the EFL suggests that the material not only provides a biocompatible substrate but also effectively transmits mechanical stress to promote membrane formation. This synovial-like layer may serve a dual purpose: preventing heterotopic ossification and creating a biological "articulation-like" interface that reduces wear particle generation. The formation of this membrane suggests potential adaptation of the biological interface, though its long-term role in mitigating wear requires further validation. Our ELISA results, showing elevated TGF-β levels, align with previous findings indicating that certain growth factors regulate SM.[31] However, as excessive SM may lead to soft-tissue hyperplasia and jeopardize long-term stability,[32] future research should focus on precisely regulating this metaplastic process to mitigate potential fibrosis and adhesion.

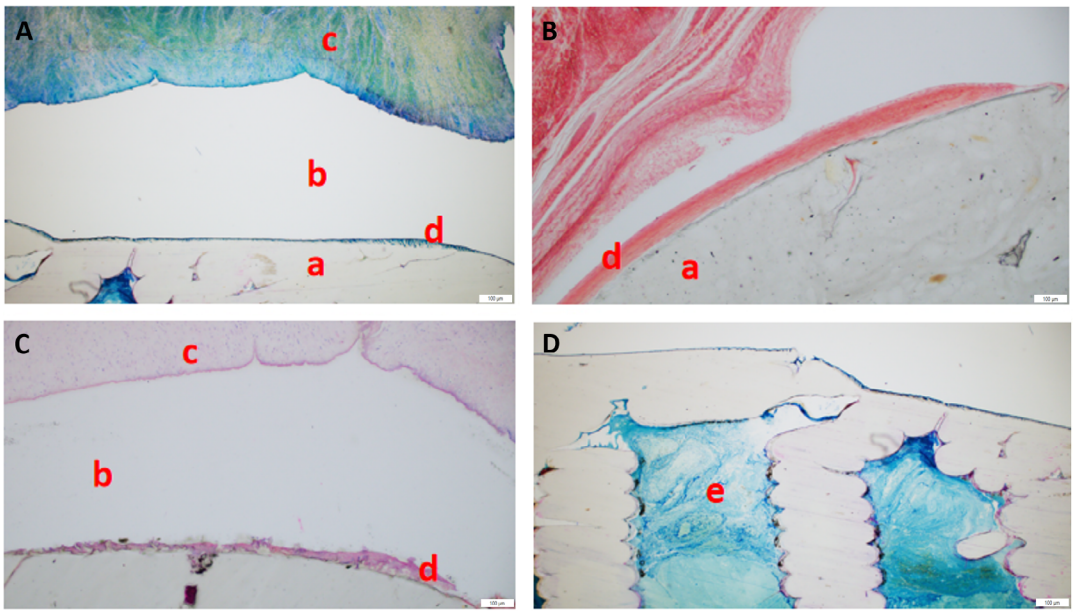

Figure 10. Histological evaluation of hard tissue sections in the prosthetic temporomandibular joint (TMJ) region. (A) Toluidine blue staining. (B) Masson's trichrome staining. (C) Hematoxylin and eosin (H&E) staining. (D) Toluidine blue staining. Representative images stained with toluidine blue, Masson's trichrome, and hematoxylin and eosin (H&E) show: (a) the porous elastic prosthesis layer; (b) the joint cavity; (c) the natural articular disc; (d) the "synovial-like" membrane formation on the prosthesis surface; (e) bone matrix ingrowth within the porous metallic scaffold. Scale bar: 100 μm; magnification: 10×.

Radiographic results at six months postoperatively confirmed that the prosthesis remained symmetrically positioned relative to the healthy joint, with no signs of dislocation or screw loosening. This underscores the robust initial stability of the elastic prosthesis. While traditional hip and knee prostheses typically last 10 to 20 years, systematic longitudinal data on TMJ prostheses are currently lacking.[33] Given our six-month observation period, longer-term follow-up is essential to establish a reliable theoretical basis for clinical translation.

A significant finding of this study is the restoration of lateral range of motion. Traditionally, total joint replacement often limits patients to vertical hinge movements, largely due to simplified bulbous socket designs and the loss of the lateral pterygoid muscle attachment.[34] Our elastic condylar prosthesis, designed with biomechanical biomimicry in mind, successfully restored lateral mandibular function, offering a critical reference for anatomical and functional reconstruction. Interestingly, while vertical and lateral mobility were effectively restored, masticatory efficiency did not fully return to preoperative levels by six months ($p < 0.05$). This discrepancy may be attributed to the surgical disruption of the masticatory musculature, particularly the lateral pterygoid muscle, or a lingering compensatory chewing pattern following unilateral surgery. Alternatively, this may be associated with temporary dysfunction of the masticatory muscle secondary to surgical trauma or postoperative compensatory occlusion, warranting long-term follow-up.[35] Furthermore, our metric for masticatory efficiency is inherently subject to behavioral confounding factors such as animal appetite and temperament. Future trials should implement more objective, biomechanical metrics, including tracking of chewing cycle counts via video analysis or direct bite-force transduction.[36] However, the stabilization of efficiency after the initial healing phase suggests a positive adaptation to the prosthesis. This is further supported by our ELISA results, which showed significantly elevated TGF-β levels in the peri-prosthetic tissues. As an essential mediator of tissue repair and synovial homeostasis, TGF-β upregulation indicates an active regenerative microenvironment that supports SM[37,38] and bone remodeling without triggering a systemic inflammatory response, as evidenced by stable hepatic and renal function metrics. However, the pleiotropic nature of TGF-β mandates caution in its interpretation. While its elevated expression correlates with protective SM and bone remodeling, chronically elevated TGF-β is a primary driver of tissue fibrosis and extracellular matrix deposition.[39] As highlighted by Ângelo *et al.*,[32] unchecked SM can progress to pathological soft-tissue hyperplasia and capsular

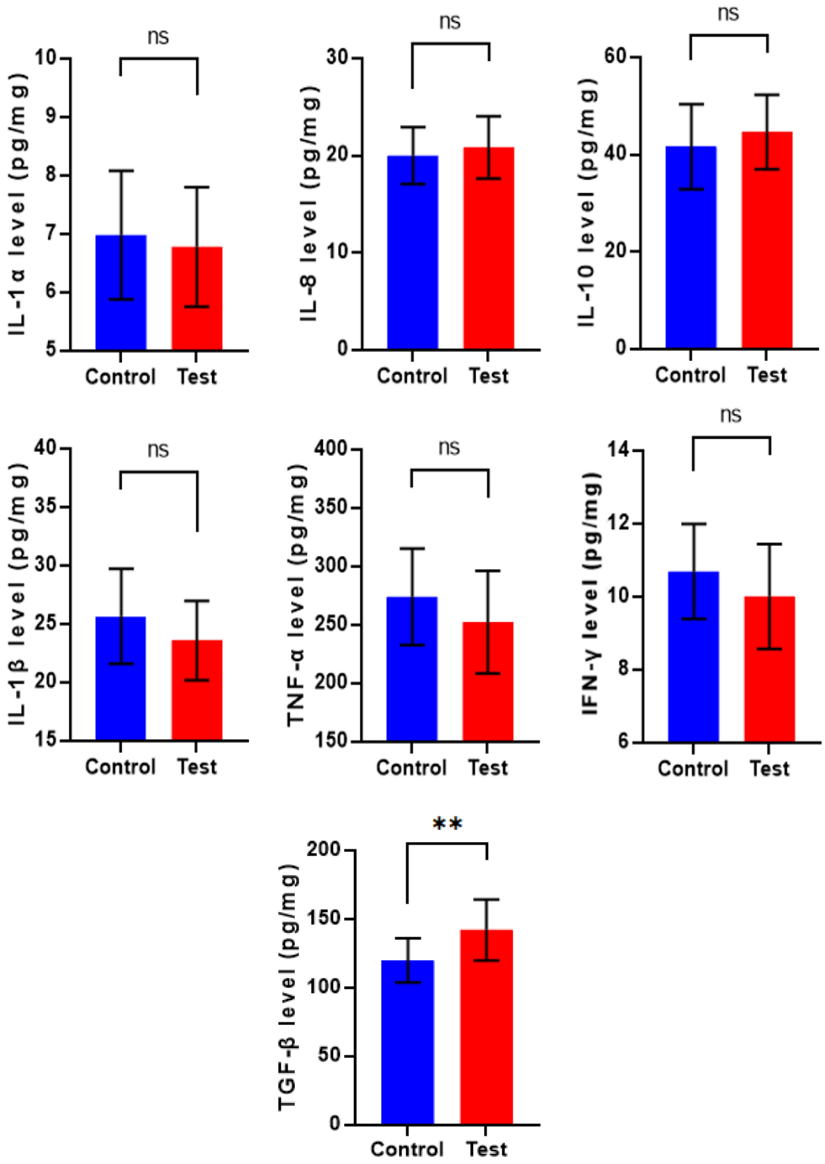

Figure 11. Local cytokine expression profiles via enzyme-linked immunosorbent assay analysis. Concentration of inflammatory cytokines (IL-1α, IL-1β, IL-8, IL-10, TNF-α, and IFN-γ) and the regenerative factor TGF-β in the peri-prosthetic tissues (Test) compared to the contralateral natural joint tissues (Control). Statistical significance was determined using paired *t*-tests. ns: $p > 0.05$; *$p < 0.05$; **$p < 0.01$.
Abbreviations: IFN-γ: Interferon gamma; IL: Interleukin; TGF-β: Transforming growth factor beta; TNF-α: Tumor necrosis factor alpha.

fibrosis, potentially restricting joint mobility over the long term. Therefore, the long-term homeostasis between TGF-β-mediated tissue repair and fibroproliferation requires vigilant longitudinal monitoring.

Current clinical protocols favor total joint replacement because rigid hemi-arthroplasty materials often induce "stress shielding" and subsequent bone resorption in the glenoid fossa. Our novel elastic design challenges this paradigm by introducing a buffering capacity that preserves the natural fossa and reduces surgical invasiveness. Despite these promising results, this study has limitations, including a relatively small sample size ($n = 4$) and a six-month observation period, which may not fully capture long-term wear characteristics. Specifically, the small cohort size may limit statistical power and increase susceptibility to individual biological variability. A post hoc power analysis revealed that,

although the statistical power for masticatory efficiency recovery reached 0.72 due to a large effect size (d = 1.76), the power for lateral excursion metrics remained below 0.50, suggesting that subtle between-group differences might have been obscured. Therefore, these pilot findings must be interpreted as preliminary trends rather than definitive statistical proof. Additionally, the lack of post-explantation surface characterization (such as scanning electron microscopy of wear tracks or remeasurement of surface roughness) is a notable omission. Because the specimens were processed *en bloc* for hard-tissue histology to preserve the bone-implant interface, the polymeric surface could not be harvested separately for tribological analysis. Future studies must allocate dedicated specimens to explicitly quantify long-term *in vivo* wear kinetics and particle debris migration.[40] Future research will focus on developing a complete "condyle–disc–fossa" elastic bionic system. We aim to provide a personalized, fully functional reconstruction that more closely mimics the complex physiological state of the human TMJ.

5. Conclusion

In conclusion, this study demonstrates that the novel 3D-printed personalized elastic bionic TMJ condylar prosthesis provides favorable initial stability, high biocompatibility, and facilitates partial functional recovery in a goat model. Notably, the elastic substrate promoted the *in vivo* formation of a "synovial-like" membrane. The formation of this membrane suggests potential adaptation of the biological interface, though its long-term role in mitigating wear and preventing heterotopic ossification requires further validation. Ultimately, our findings supply robust preclinical validation for the integration of elastic designs in the next generation of TMJ arthroplasty.

Acknowledgments

None.

Funding

This work was supported by grants from Beijing Natural Science Foundation (L242059).

Conflict of interest

The authors declare they have no competing interests.

Author contributions

Conceptualization: Junqi Jiang, Xiangliang Xu, Chuanbin Guo
Formal analysis: Kenan Chen, Junlin Wang, Bingxue Cheng
Investigation: Junqi Jiang, Zhiwei Jiao, Kenan Chen, Junlin Wang, Bingxue Cheng
Methodology: Qingxiang Li, Zhiwei Jiao
Writing–original draft: Junqi Jiang, Qingxiang Li
Writing–review & editing: Xiangliang Xu, Chuanbin Guo

Ethics approval and consent to participate

All procedures were approved by the Institutional Animal Care and Use Committee of Peking University School of Stomatology (Approval No. LA2020286) and were conducted in strict accordance with national guidelines for the care and use of laboratory animals.

Consent for publication

Not applicable.

Availability of data

Data are available from the corresponding authors upon reasonable request.

References

1. Yoda T, Ogi N, Yoshitake H, *et al*. Clinical guidelines for total temporomandibular joint replacement. *Jpn Dent Sci Rev.* 2020;56(1):77-83.

   doi: 10.1016/j.jdsr.2020.03.001

2. Thor A, Bengtsson M, Dowgierd K, *et al*. Alloplastic total temporomandibular joint (TMJ) replacement registry: a protocol for a prospective global multicentre observational cohort study. *BMJ Open.* 2026;16(3):e113558.

   doi: 10.1136/bmjopen-2025-113558

3. De Meurechy N, Braem A, Mommaerts M Y. Biomaterials in temporomandibular joint replacement: current status and future perspectives-a narrative review. *Int J Oral Maxillofac Surg.* 2018;47(4):518-533.

   doi: 10.1016/j.ijom.2017.10.001

4. Cheng KJ, Liu YF, Wang JH, *et al*. 3D-printed porous condylar prosthesis for temporomandibular joint replacement: Design and biomechanical analysis. *Technol Health Care.* 2022;30(4):1017-1030.

   doi: 10.3233/THC-213534

5. Piao C, Wu D, Luo M, Ma H. Stress shielding effects of two prosthetic groups after total hip joint simulation replacement. *J Orthop Surg Res.* 2014;9(1):17.

   doi: 10.1186/s13018-014-0071-x

6. Kent JN, Misiek DJ, Akin RK, Hinds EC, Homsy CA. Temporomandibular joint condylar prosthesis: a ten-year report. *J Oral Maxillofac Surg.* 1983;41(4):245-254.

   doi: 10.1016/0278-2391(83)90267-7

7. Elledge R, Mercuri LG, Attard A, Green J, Speculand B. Review of emerging temporomandibular joint total joint replacement systems. *Br J Oral Maxillofac Surg.*

2019;57(8):722-728.

doi: 10.1016/j.bjoms.2019.08.009

8. Niezen ET, van Minnen B, Bos RRM, Dijkstra PU. Temporomandibular joint prosthesis as treatment option for mandibular condyle fractures: a systematic review and meta-analysis. *Int J Oral Maxillofac Surg.* 2023;52(1):88-97.

doi: 10.1016/j.ijom.2022.05.014

9. Mehrotra D, Kumar S, Mehrotra P, *et al*. Patient specific total temporomandibular joint reconstruction: A review of biomaterial, designs, fabrication and outcomes. *J Oral Biol Craniofac Res.* 2021;11(2):334-343.

doi: 10.1016/j.jobcr.2021.02.014

10. Zheng JS, Liu XH, Chen XZ, *et al*. Customized skull base-temporomandibular joint combined prosthesis with 3D-printing fabrication for craniomaxillofacial reconstruction: a preliminary study. *Int J Oral Maxillofac Surg.* 2019;48(11):1440-1447.

doi: 10.1016/j.ijom.2019.02.020

11. Stanković S, Vlajković S, Bošković M, Radenković G, Antić V, Jevremović D. Morphological and biomechanical features of the temporomandibular joint disc: an overview of recent findings. *Arch Oral Biol.* 2013;58(10):1475-1482.

doi: 10.1016/j.archoralbio.2013.06.014

12. Jiang N, Chen H, Zhang J, *et al*. Decellularized-disc based allograft and xenograft prosthesis for the long-term precise reconstruction of temporomandibular joint disc. *Acta Biomater.* 2023;159:173-187.

doi: 10.1016/j.actbio.2023.01.042

13. Zhao J, Dai H, Qiao K, *et al*. Viscoelastic Polyurethane Discs with Host-Guest Interaction for Temporomandibular Joint Function Restoration. *Adv Funct Mater*. 2026;36(8):e07926.

doi: 10.1002/adfm.202507926

14. Xu X, Zhang J, Luo D, Guo C, Rong Q. Biomechanical comparison between the custom-made mandibular condyle prosthesis and total temporomandibular joint prosthesis in finite element analysis. *Acta Bioeng Biomech*. 2020;22(4): 151-160.

doi: 10.37190/ABB-01721-2020-03

15. Guo F, Huang S, Hu M, Yang C, Li D, Liu C. Biomechanical evaluation of a customized 3D-printed polyetheretherketone condylar prosthesis. *Exp Ther Med*. 2021;21(4):348.

doi: 10.3892/etm.2021.9779

16. Ackland DC, Robinson D, Redhead M, Lee PVS, Moskaljuk A, Dimitroulis G. A personalized 3D-printed prosthetic joint replacement for the human temporomandibular joint: From implant design to implantation. *J Mech Behav Biomed Mater.* 2017;69:404-411.

doi: 10.1016/j.jmbbm.2017.01.048

17. Jiang J, Jiao Z, Cheng B, Han J, Xu X, Guo C. Design, fabrication, and evaluation of a novel 3D-printed temporomandibular joint prosthesis enhanced with elastic layer. *Int J Bioprinting*. 2024;0(0):4899.

doi: 10.36922/ijb.4899

18. Baecher H, Maheta B, Lottner LM, *et al*. Current clinical and translational challenges in temporomandibular joint reconstruction. *Front Bioeng Biotechnol.* 2025;18(13):1590021.

doi: 10.3389/fbioe.2025.1590021

19. Angelo DF, Morouço P, Alves N, *et al*. Choosing sheep (Ovis aries) as animal model for temporomandibular joint research: Morphological, histological and biomechanical characterization of the joint disc. *Morphologie*. 2016;100(331):223-233.

doi: 10.1016/j.morpho.2016.06.002

20. Mommaerts MY, Deman F, Verwilghen D, De Meurechy N. Lateral pterygoid muscle enthesis reconstruction in alloplastic total temporomandibular joint replacement: an animal experiment with histological verification. *J Craniomaxillofac Surg*. 2025;53(5):476–483.

doi: 10.1016/j.jcms.2025.01.022

21. Xu X, Luo D, Guo C, Rong Q. A custom-made temporomandibular joint prosthesis for fabrication by selective laser melting: Finite element analysis. *Med Eng Phys.* 2017;46(1):1-11.

doi: 10.1016/j.medengphy.2017.04.012

22. Shokrgozar MA, Farokhi M, Rajaei F, *et al*. Biocompatibility evaluation of HDPE-UHMWPE reinforced β-TCP nanocomposites using highly purified human osteoblast cells. *J Biomed Mater Res A*. 2010;95A(4):1074-1083.

doi: 10.1002/jbm.a.32892

23. Shen P, Zhang SY, Yang C, Yun B. Biological safety evaluation of total temporomandibular joint prosthesis in sheep. *China J Oral Maxillofac Surg.* 2013,11(4):297-302.

doi: CNKI:SUN:ZGKQ.0.2013-04-009.

24. Shen P, Zhang SY, Yang C, Yun B. Stability study of total temporomandibular joint replacement on sheep. *J Craniomaxillofac Surg.* 2014;42(7):1265-1270.

doi: 10.1016/j.jcms.2014.03.008

25. Trento G, Parize H, Bohner L, Oelerich O, Jung S, Kleinheinz J. Can a unilateral total temporomandibular joint prosthesis affect the healthy contralateral temporomandibular joint? A systematic review. *Int J Oral Maxillofac Surg.* 2025;54(1):65-73.

doi: 10.1016/j.ijom.2024.10.001.

26. Olate S, Ravelo V, Huentequeo C, Parra M, Unibazo A. An Overview of Clinical Conditions and a Systematic Review of Personalized TMJ Replacement. *J Pers Med*. 2023;13(3):533.

doi: 10.3390/jpm13030533

27. Monje F, Mercuri L, Villanueva-Alcojol L, de Mera JJ. Synovial metaplasia found in tissue encapsulating a silicone spacer during 2-staged temporomandibular joint replacement for ankylosis. *J Oral Maxillofac Surg*. 2012;70(10):2290-2298.

    doi: 10.1016/j.joms.2012.06.177

28. Raso DS, Greene WB, Harley RA, Maize JC. Silicone deposition in reconstruction scars of women with silicone breast implants. *J Am Acad Dermatol*. 1996;35(1):32-36.

    doi: 10.1016/S0190-9622(96)90492-2

29. Ko CY, Ahn CY, Ko J, Chopra W, Shaw WW. Capsular synovial metaplasia as a common response to both textured and smooth implants. *Plast Reconstr Surg*. 1996;97(7):1427-1433.

    doi: 10.1097/00006534-199606000-00017

30. Drachman D B, Sokoloff L. The role of movement in embryonic joint development. *Dev Biol*. 1966;14(3): 401-420.

    doi: 10.1016/0012-1606(66)90022-4

31. Linden O, Kelil T, Greenwood H, Lauw M, Strachowski L. Capsular synovial metaplasia mimicking radiographic features of implant-associated anaplastic lymphoma. *Clin Imaging*. 2020;59(2):144-147.

    doi: 10.1016/j.clinimag.2019.10.019

32. Ângelo DF, Cardoso HJ, Sanz D. Synovial entrapment in alloplastic temporomandibular joint replacement. *Int J Oral Maxillofac Surg*. 2021;50(12):1628-1631.

    doi: 10.1016/j.ijom.2021.05.022

33. Vargas E, Ravelo V, Rana M, Unibazo A, Olate S. Long-Term Stability in Temporomandibular Joint Replacement: A Review of Related Variables. *Dent J (Basel)*. 2024;12(11):372.

    doi: 10.3390/dj12110372

34. Zhong YQ, Sun Q, He DM, Zou LX, Lu C. Study on the lateral pterygoid muscle status after artificial temporomandibular joint replacement. *Int J Oral Maxillofac Surg*. 2021;50(11):1496-1501.

    doi: 10.1016/j.ijom.2021.03.008

35. Su L, Kang Y, Guo C, Wang X. Analysis of Dynamic Mandibular Movement of Patients With Condylar Hyperplasia Treated With Orthognathic Surgery and Condylectomy. *J Craniofac Surg*. 2025;36(6):1972-1977.

    doi: 10.1097/SCS.0000000000011083

36. Lall AB, Singhal M, Kusum T, Safi S. Evaluation of Masticatory Efficiency and Mandibular Function Following Open or Closed Reduction of Mandibular Fractures. *J Maxillofac Oral Surg*. 2025;24(6):1668-1675.

    doi: 10.1007/s12663-025-02641-x.

37. Braczkowski MJ, Kufel KM, Kulińska J, *et al*. Pleiotropic Action of TGF-β in Physiological and Pathological Liver Conditions. *Biomedicines*. 2024;12(4):925.

    doi: 10.3390/biomedicines12040925

38. de Araújo Farias V, Carrillo-Gálvez AB, Martín F, Anderson P. TGF-β and mesenchymal stromal cells in regenerative medicine, autoimmunity and cancer. *Cytokine Growth Factor Rev*. 2018;43:25-37.

    doi: 10.1016/j.cytogfr.2018.06.002

39. Nakerakanti S, Trojanowska M. The Role of TGF-β Receptors in Fibrosis. *Open Rheumatol J*. 2012;6(1):156-162.

    doi: 10.2174/1874312901206010156

40. De Meurechy N, Aktan MK, Boeckmans B, *et al*. Surface wear in a custom manufactured temporomandibular joint prosthesis. *J Biomed Mater Res B Appl Biomater*. 2022;110(6):1425-1438.

    doi: 10.1002/jbm.b.35010